Available online at www.sciencedirect.com
ScienceDirect
Ceramics International 35 (2009) 1851–1854
CERAMICS INTERNATIONAL
www.elsevier.com/locate/ceramint

Mechanical and dielectric properties of porous Si_2N_2O–Si_3N_4 in situ composites

Li ShuQin [a,*], Pei YuChen [b], Yu ChangQing [a], Li JiaLu [b]

[a] *Institute 306th, China Aerospace Science and Industry Corporation, Beijing 7203#-21, 100074, People's Republic of China*
[b] *Composite Research Institute, Tianjin Polytechnic University, Tianjin 300160, People's Republic of China*

Received 3 June 2008; received in revised form 24 June 2008; accepted 10 October 2008
Available online 17 November 2008

Abstract

Mechanical and dielectric properties of porous Si_2N_2O–Si_3N_4 in situ composites fabricated for use as radome by gel-casting process were investigated. The flexural strength of the Si_2N_2O–Si_3N_4 ceramics is 230.46 ± 13.24 MPa, the complex permittivity of the composites varies from 4.34 to 4.59 and the dissipation factor varies from 0.00053 to 0.00092 from room temperature to elevated temperature (1150 °C) at the X-band. In the porous regions, some Si_2N_2O fibers (50–100 nm in diameter) are observed which may improve the materials properties.

Keywords: A. Shaping; B. Composites; B. Electron microscopy; B. Porosity

1. Introduction

Silicon nitride (Si_3N_4) ceramics is a suitable material for high temperature radome application because of the high temperature mechanical strength, good resistance to corrosion, low dielectric constant and loss, good thermomechanical property [1–9]. On the other hand, the silicon oxynitride (Si_2N_2O) ceramics have been recognized as a promising material for high temperature applications due to their good resistant to oxidation and to thermal shock [10,11]. The silicon oxynitride phase shows the development of elongated grains which can be used to toughen silicon nitride when properly dispersed. Si_2N_2O can optimize the properties of silicon nitride based ceramics [12].

The Si_2N_2O–Si_3N_4 ceramics were studied by many researchers on the properties, however, which mostly focused on the mechanical property of the materials. The dielectric property of the material which used as radome is considerable important. So, porous Si_2N_2O–Si_3N_4 in situ composites were fabricated using gel-casting process in this work. Pores were introduced into ceramics because the dielectric constant of the materials decreased with the increase of porosity which was very beneficial to radome design. The microstructures of the Si_2N_2O–Si_3N_4 ceramics were studied and the formation of Si_2N_2O fibers in the pores as well as the matrix was investigated. The mechanical and dielectric properties of porous Si_2N_2O–Si_3N_4 ceramics were reported.

2. Experimental procedure

2.1. Raw materials

As starting materials, the Si_3N_4 powder (Beijing Tsinghua Unisp Lendor High Technology Ceramics Co., China. d_{50} = 0.5 μm, α phase 93%), the SiO_2 (Chengdu Sinuowei Co., Ltd., China. d_{50} = 2 μm, purify 99.95%) and sintering additives (Yb_2O_3 and Al_2O_3, Yb_2O_3 Griem Advanced Materials Co., Ltd.; Al_2O_3 Zibo Hengji Tianli Co., Ltd., China.) for the mixed AM–MBAM system were listed in Table 1.

2.2. Preparation of suspensions

The schematic forming process of gel-casting was described in Fig. 1. First, the mixture powder of 80 wt% α-Si_3N_4, 10 wt% SiO_2, 6 wt% Yb_2O_3 and 4 wt% Al_2O_3 powder and 0.25 wt% dispersant were added to premix solution of organic monomer by mechanical stirring till solids loading up to 45 vol.%. Afterwards, the mixtures were milled for 24 h in a nylon resin

* Corresponding author. Tel.: +86 10 68190540; fax: +86 10 88534479.
E-mail address: lishuqin97@hotmail.com (L. ShuQin).

0272-8842/$34.00
doi:10.1016/j.ceramint.2008.10.021

Table 1
Raw materials for the AM–MBAM system.

Function	Raw material	Manufacturer
Monomer	Acrylamide (AM)	Aldrich, USA
Crosslinker	N,N′-methylenebisacrylamide (MBAM)	Hongxing Biological and Chemical Factory of Beijing, China
Catalyst	N,N,N′N′-tetramethylethylenediamine (TEMED)	Beijing Chemical Reagent Company, China
Initiator	Ammonium persulphate (APS)	Beijing Third Reagent Works, China
Dispersant	Tetramethylammoniumhydoxide solution	Beijing Chemical Reagent Company, China
Solvent	Deionized water	

jar using alumina ball-milling media to break down agglomerates and to achieve good homogeneity. After degassing for 8–10 min in a rotary evaporator under vacuum, the initiator and catalyst were applied to the slurry. Then it was cast into metal mould at room temperature. Afterwards the mould was moved into an oven at temperature of 60–80 °C, and the consolidation of suspension formed a green body. After consolidation, the green bodies were demolded and dried under controlled humidity to avoid cracking and non-uniform shrinkage due to rapid drying. Binder burnout was operated at 600 °C for 2 h, with a heating rate of 2 °C/min and a natural cooling. Then the samples were embedded in 50 wt% Si_3N_4 + 40 wt% BN + 10 wt% Al_2O_3 powder bed in a graphite crucible and sintered to the temperature of 1680 °C for 1.5 h in N_2 atmosphere, followed by natural cooling under N_2 gas atmosphere.

The flexural strengths of bars of green and sintered bodies were examined by three-point flexure test with a span of 30 mm at a loading rate of 0.5 mm/min. The bars of green and sintered bodies were 5 mm × 6 mm × 42 mm and 3 mm × 4 mm × 36 mm, respectively. Six samples were used to calculate the average values and errors. For the measurements of dielectric properties, three specimens with the dimensions of approximately φ 54 mm × 3 mm were prepared from the center part of each sample. Complex permittivity (ε) and dissipation factor ($\tan\delta$) were measured at high frequency from room temperature to 1150 °C by the perturbation method using a cavity resonator and a vector network analyzer. To identify the phase of the samples, XRD (Cu Kα, D/MAX-250, Rigaku, Japan) technique was employed on the polished surfaces. Meanwhile, microstructure analysis of the surfaces of the samples, which were polished with diamond pastes and etched with melting NaOH at 400 °C for 1.5 min, was carried out by scanning electron microscopy (SEM). The microstructure, pore size, pore distribution and morphology of the fibers in the porous Si_2N_2O–Si_3N_4 bodies of the cross-section were observed by SEM.

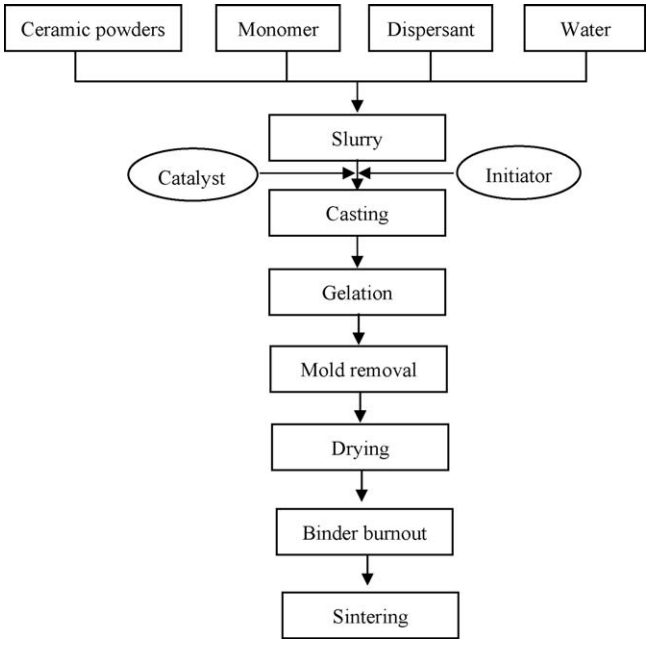

Fig. 1. The gel-casting process flow chart.

3. Results and discussion

3.1. The Si_2N_2O phase formation

Fig. 2 shows the XRD profiles of the sample. It can be revealed that the Si_3N_4 as well as Si_2N_2O phases are all existed. Formation of silicon oxynitride can be explained according to two possibilities. The first one is related to the oxidation of the Si_3N_4 phase, in accordance with the following reaction:

$$2Si_3N_4(s) + (3/2)O_2(g) \rightarrow 3Si_2N_2O(s) + N_2(g) \quad (1)$$

If there exists oxygen which comes from the N_2 atmosphere, Si_3N_4 is thermodynamically unstable with respect to oxidation. Even though it has excellent high temperature mechanical properties, it suffers from poor oxidation resistance at high temperatures. Moreover, although thermodynamically reaction

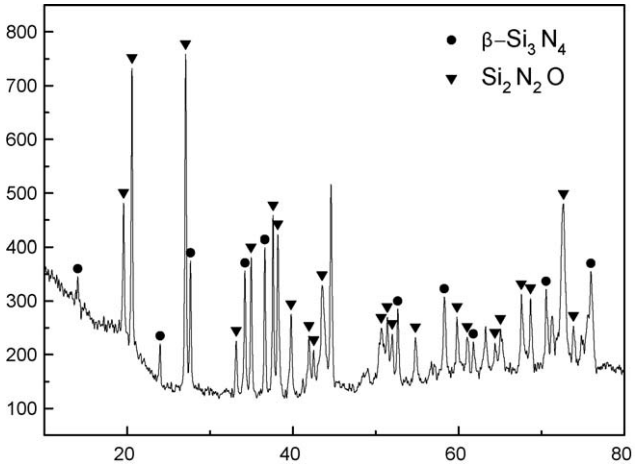

Fig. 2. The XRD profiles of the sample.

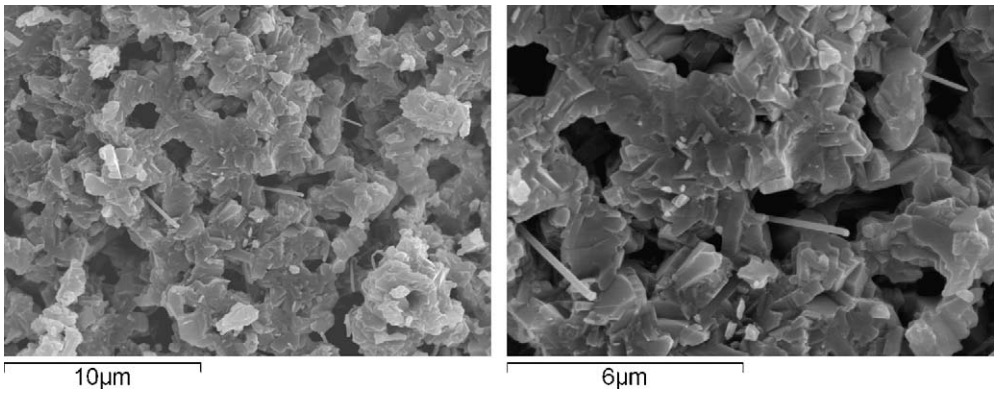

Fig. 3. SEM fracture surfaces of the Si_2N_2O–Si_3N_4 composites.

(1) is high feasible (for instance, at 1500 K, $\Delta G_R = -1063$ kJ/mol), the oxidation of Si_3N_4 occurs slowly, following approximately a kinetics with parabolic behavior. Once oxidation has occurred, the oxide film formed serves as a protection against catastrophic oxidation by precluding the transport of oxygen atoms through the nitride surface. In fact, passive oxidation and the ability of Si_3N_4 to resist high temperatures under oxidizing conditions rely on the integrity and stability of the oxide layer in the surface. The second possibility is the reaction between Si_3N_4 and SiO_2 according to

$$SiO_2(l) + Si_3N_4(s) \rightarrow 2Si_2N_2O(s) \quad (2)$$

In the present material, Si_2N_2O grows via a solution-precipitation process in the presence of a large amount of SiO_2-rich liquid phase. Obviously, the liquid phases are largely consumed with the formation of the crystalline Si_2N_2O.

3.2. The microstructure and the mechanical and dielectric properties

Fig. 3 shows SEM fracture surfaces of the Si_2N_2O–Si_3N_4 composites. The pore is distributed evenly in the matrix and the diameter of the pore is about 3 μm. In the porous microstructure, it can be seen that the irregular shaped fibers extend from the pore. The diameter of the fibers is about 50–100 nm. No droplet is observed on the tip of the fibers. This observation indicates that Si_2N_2O fibers can be formed through the vapor–solid (VS) reaction between SiO and N_2 during the sintering process [13]. However, some Si_2N_2O fibers show wavy and rough surface due to the formation of several nucleation sites.

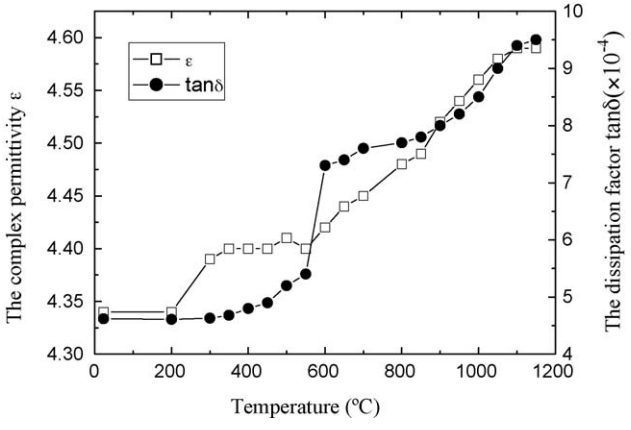

Fig. 4. The relationship between the complex permittivity and the dissipation factor and temperature.

The flexural strengths of the green sample and the sintered sample are 30.22 ± 1.58 MPa and 230.46 ± 13.24 MPa, respectively. It can be seen that it possesses the appropriate flexural strength as the radome material. The material properties of the greatest importance to microwave interaction of a dielectric are the complex permittivity, $\varepsilon = \varepsilon' - j\varepsilon''$, and the dissipation factor, $\tan\delta = \varepsilon''/\varepsilon'$. The real part ($\varepsilon'$) correlates with polarization, and the imaginary part (ε'') represents dielectric loss; the dissipation factor ($\tan\delta$) predicts the ability of the material to convert the absorbed electromagnetic energy into heat. The complex permittivity and the dissipation factor changing with the temperature are shown in Fig. 4.

The results show that the complex permittivity of the composites varies from 4.34 to 4.59 and the dissipation factor varies from 0.00046 to 0.00095 when the temperature rises from room to elevated (1150 °C) at the X-band. The complex permittivity and the dissipation factor of the composite specimens increase with increasing the temperature. The microstructure features that influence mechanical properties of ceramics also influence electrical properties. The porosity decreases the strength of a ceramic, meanwhile, it also decreases the complex permittivity. The formula used in the complex permittivity as a function of percent pores is $\varepsilon = \varepsilon_0^{1-P}$, where ε_0 is the complex permittivity of the 100% dense material and P is the volume fraction of pores. Due to the pores, the dielectric properties of the Si_2N_2O–Si_3N_4composite are excellent.

4. Conclusions

Porous Si_2N_2O–Si_3N_4 ceramics were fabricated for use as radome by gel-casting process and pressureless sintering were investigated. Some Si_2N_2O fibers (50–100 nm in diameter) are formed through the vapor–solid reaction between SiO and N_2 during the sintering process. The flexural strength of the Si_2N_2O–Si_3N_4 ceramics is 230.46 ± 13.24 MPa and the

complex permittivity of the composites varies from 4.34 to 4.59 and the dissipation factor varies from 0.00053 to 0.00092 when the temperature rises from room to elevated (1150 °C) at the X-band. Mechanical and dielectric properties of the Si_2N_2O–Si_3N_4composite are excellent.

References

[1] Y. Inagaki, O.T. Kondon, High performance porous silicon nitrides, J. Eur. Ceram. Soc. 22 (2002) 2489–2494.

[2] T. Ohji, Y. Shigegaki, T. Miyajima, S. Kanzaki, Fracture resistance behavior of multilayered silicon nitride, J. Am. Ceram. Soc. 80 (1997) 991–994.

[3] J.H. She, J.F. Yang, D.D. Jayaseelan, N. Kondo, T. Ohji, S. Kanzaki, Y. Inagaki, Thermal shock behavior of isotropic and anisotropic porous silicon nitride, J. Am. Ceram. Soc. 86 (2003) 738–740.

[4] S.K. Lee, J.D. Moretti, M.J. Readey, B.R. Lawn, Thermal shock resistance of silicon nitrides using an indentation-quench test, J. Am. Ceram. Soc. 85 (2002) 279–281.

[5] T. Sekine, Shock synthesis of cubic silicon nitride, J. Am. Ceram. Soc. 85 (2002) 113–116.

[6] D.S. Fox, E.J. Opila, Q.N. Nguyen, D.L. Humphrey, S.M. Lewton, Para-linear oxidation of silicon nitride in a water–vapor/oxygen environment, J. Am. Ceram. Soc. 86 (2003) 1256–1261.

[7] M. Backhaus-Ricoult, V. Guerin, A.M. Huntz, V.S. Urbanovich, High-temperature oxidation behavior of high-purity alpha-, beta-, and mixed silicon nitride ceramics, J. Am. Ceram. Soc. 85 (2002) 385–392.

[8] Y. Zhang, Y.B. Cheng, S. Lathabai, K. Hirao, Erosion response of highly anisotropic silicon nitride, J. Am. Ceram. Soc. 88 (2005) 114–120.

[9] A. Zerr, M. Kempf, M. Schwarz, E. Kroke, M. Goken, R. Riedel, Elastic moduli and hardness of cubic silicon nitride, J. Am. Ceram. Soc. 85 (2002) 86–90.

[10] M. Radwan, T. Kashiwagi, Y. Miyamoto, New synthesis route for Si_2N_2O ceramics based on desert sand, J. Eur. Ceram. Soc. 23 (2003) 2337–2341.

[11] X. Rong-Jun, M. Mamoru, X. Fang-Fang, Z. Guo-Dong, B. Yoshio, A. Yoshio, Microstructure and mechanical properties of superplastically deformed silicon nitride–silicon oxynitride in situ composites, J. Eur. Ceram. Soc. 22 (2002) 963–971.

[12] H. Emoto, M. Mitomo, C.M. Wang, H. Hirosturu, T. Inaba, Fabrication of silicon nitride–silicon oxynitride in situ composites, J. Eur. Ceram. Soc. 18 (1998) 527–533.

[13] B. Lee, R.K. Paul, C.W. Lee, H.D. Kim, Fabrication and microstructure characterization of continuously porous Si_2N_2O–Si_3N_4 ceramics, Mater. Lett. 61 (11–12) (2007) 2182–2186.